

Isoapoptolidin: Structure and Activity of the Ring-Expanded Isomer of Apoptolidin

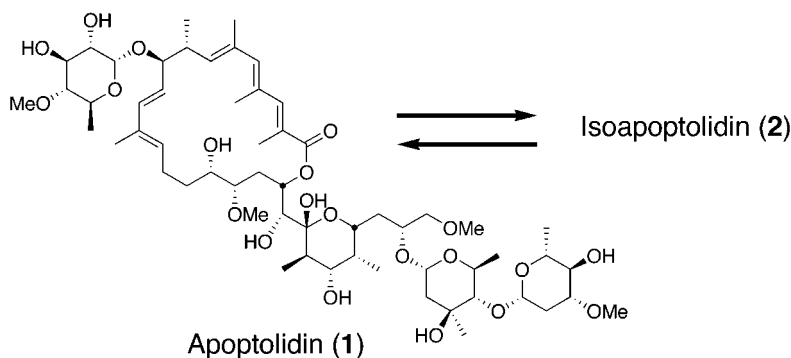
Paul A. Wender,^{*,†} Aaron V. Gulledge,[†] Orion D. Jankowski,[†] and Haruo Seto[‡]

Department of Chemistry, Stanford University, Stanford, California 94305-5080, and
Molecular and Cellular Biosciences, University of Tokyo, Japan

wenderp@stanford.edu

Received July 27, 2002

ABSTRACT



Apoptolidin (1) is a novel oncolytic lead that induces apoptosis in transformed cell lines with exceptional selectivity. We report the isolation and characterization of a ring-expanded macrolide isomer of apoptolidin: isoapoptolidin (2). The solution conformation of isoapoptolidin is described. The rate of isomerization was measured under biologically relevant conditions and found to approach equilibrium within the time frame of most cell-based assays. Isoapoptolidin's ability to inhibit mitochondrial F_0F_1 -ATPase is over 10-fold less than that of apoptolidin.

In 1997, Seto and co-workers¹ reported the structure of apoptolidin (1), which was isolated from *Nocardopsis* sp. in a screening program designed to identify new compounds that selectively induce apoptosis in E1A-transformed cells. In the National Cancer Institute's 60 human cancer cell line assay, apoptolidin was found to be among the top 0.1% most selective agents of the more than 37 000 compounds analyzed to date.^{2,3} The ability of apoptolidin to induce apoptosis in transformed cells with such remarkable selectivity represents an exciting new lead strategy for the treatment of cancer. The Khosla group recently identified mitochondrial F_0F_1 -ATPase as a cellular target of apoptolidin and further demonstrated that cell lines that were unresponsive to

treatment with apoptolidin could be sensitized by cotreatment with either oxamate or 2-deoxyglucose.³ Despite this, the basis for apoptolidin's selectivity against different cell lines is not well understood.

Apoptolidin's important biological activity and complex structure have made it a popular target for total synthesis.⁴ An alternative approach to establishing the structural basis for apoptolidin's activity and for identifying related clinical leads is modification of apoptolidin itself, available in substantial quantity (109 mg/L) through fermentation.¹ As part of our efforts in this direction, we have identified an

[†] Stanford University.

[‡] University of Tokyo.

(1) (a) Kim, J. W.; Adachi, H.; Shin-ya, K.; Hayakawa, Y.; Seto, H. *J. Antibiotics* **1997**, 50, 628. (b) Hayakawa, Y.; Kim, J. W.; Adachi, H.; Shin-ya, K.; Fujita, K.; Seto, H. *J. Am. Chem. Soc.* **1998**, 120, 3524.

(2) Developmental Therapeutics Program NCI/NIH. <http://dtp.nci.nih.gov> (accessed July 2002).

(3) (a) Salomon, A. R.; Voehringer, D. W.; Herzenberg, L. A.; Khosla, C. *Proc. Natl. Acad. Sci. U.S.A.* **2000**, 97, 14766. (b) Salomon, A. R.; Voehringer, D. W.; Herzenberg, L. A.; Khosla, C. *Chem. Biol.* **2001**, 8, 71. (c) Salomon, A. R.; Zhang, Y.; Seto, H.; Khosla, C. *Org. Lett.* **2001**, 3, 57.

Table 1. ^{13}C (100 MHz) and ^1H (500 MHz) NMR Data for Isoapoptolidin in CD_3OD

isoapoptolidin (2)				apoptolidin (1) ¹			
no.	δ_{C}	δ_{H} ($J = \text{Hz}$)	δ_{H}	no.	δ_{C}	δ_{H} ($J = \text{Hz}$)	δ_{H}
1	169.92			2-Me	13.92	2.04	2.14
2	124.86			4-Me	17.82	2.07	2.21
3	147.08	7.31	7.41	6-Me	17.63	1.72 (1.0)	1.97
4	132.76			8-Me	18.26	1.17 (6.4)	1.17
5	143.65	5.93	6.23	12-Me	12.00	1.70	1.71
6	132.90			17-OMe	59.87	3.47	3.40
7	136.75	5.06 (9.1)	5.27	22-Me	12.13	1.03 (6.7)	1.06
8	39.41	2.74	2.79	24-Me	5.38	0.86 (6.9)	0.92
9	83.98	3.77 (9.0, 9.0)	3.87	28-OMe	59.48	3.35	3.30
10	125.77	5.26 (15.8, 9.0)	5.26	1'	96.23	4.78 (3.8)	4.85
11	141.01	6.04 (15.8)	6.21	2'	73.32	3.38 (9.8, 3.8)	3.44
12	134.05			3'	74.92	3.71	3.76
13	133.80	5.48 (9.6, 4.8)	5.71	4'	87.53	2.70 (9.0)	2.76
14 α	25.49	1.93	2.09	5'	68.05	3.73	3.78
14 β		2.48	2.50	6'	18.38	1.22 (6.2)	1.29
15 α	33.37	1.24	1.44	4'-OMe	61.01	3.56	3.61
15 β		1.39	1.52	1''	99.88	5.05 (4.1)	4.97
16	73.10	3.51 (10.3, 5.0, 2.3)	3.47	2'' α	45.29	2.01	1.96
17	81.89	3.36	2.75	2'' β		1.77	1.84
18 α	35.05	1.36	1.78	3''	73.67		
18 β		1.84	2.20	4''	85.91	3.32	3.37
19	67.44	4.41 (11.3, 3.7, 2.1)	5.32	5''	68.62	3.73	3.70
20	74.13	4.98 (3.7)	3.57	6''	18.35	1.22 (6.2)	1.25
21	103.27			3''-Me	22.76	1.34	1.36
22	36.79	1.77	2.08	1'''	101.91	4.82 (9.7, 1.8)	4.86
23	73.20	3.72	3.76	2''' α	37.15	2.43 (12.3, 5.0, 1.8)	2.47
24	40.52	1.74	1.76	2''' β		1.28	1.32
25	68.17	4.21 (10.3, 2.5, 2.0)	3.99	3'''	81.98	3.16 (11.6, 9.0, 5.0)	3.21
26 α	36.82	1.76	1.62	4'''	77.12	2.95 (9.0, 9.0)	3.01
26 β		1.53 (14.7, 10.7, 3.0)	1.49	5'''	73.45	3.19	3.24
27	76.24	3.82	3.48	6'''	18.87	1.27 (6.2)	1.31
28	77.07	3.44	3.36	3'''-OMe	57.32	3.42	3.46

isomer of apoptolidin and report herein its characterization, solution conformation, and biological activity.

Our initial attempts to isolate apoptolidin from crude cell extracts were complicated by the presence of an isomer, referred to herein as isoapoptolidin (**2**), that coeluted during chromatography. It was found that apoptolidin can be partially separated from this isomer, which has a slightly lower R_f on normal-phase silica, by flash column chromatography.⁵ Isoapoptolidin, however, remained impure, even after subsequent attempts to isolate it using either normal-phase or reverse-phase HPLC. Surprisingly, an enriched solution of **2** in either chloroform or acetonitrile was found to produce pure **2** over several hours at room temperature as white filamentous crystals (mp 134–136 °C). These crystals of **2**, unfortunately, have thus far proven to be unsuitable for X-ray analysis because of their poor aspect ratio. This crystallization takes place even from very dilute solutions of **2** but does not occur when **1** is present in substantial amounts. Mass recovery of **1** and **2** from crude cell extracts indicates that the two isomers are present in roughly equal amounts.

The structure of **2** was determined by analysis of one- and two-dimensional NMR spectra (500 MHz). In CD_3OD , the

chemical shifts of most proton signals in **2** remain very similar to those reported by Seto and co-workers for apoptolidin.¹ The same spin systems found in **1** were also present in **2**, as determined by DQF-COSY experiments. The HMBC spectrum of **2**, however, shows a strong correlation between the carbonyl carbon (C-1) and 20-H. In addition, the chemical shift of 20-H is shifted downfield, from 3.57 ppm in **1** to 4.98 ppm in **2**, strongly suggesting that it is now geminal to the lactone functionality. Similarly, 19-H shifts upfield, from 5.32 ppm in **1** to 4.41 ppm in **2**. All the proton and carbon resonances have been assigned for **2** in CD_3OD and are summarized in Table 1.

Strong ROESY correlations between 1,3-diaxial substituents on the C-21 to C-25 cyclic hemiketal in **2** indicate that it is in a chairlike conformation. ROESY correlations are observed from 20-H to both 22-H and 22-Me- H_3 , indicating that C-20 is equatorial on the ring. Coupling constant data for the anomeric proton signals (Table 1) indicate that the stereochemistry of the glycosidic bonds in **2** remain the same as those found in **1**. Finally, high-field carbon chemical shift for the allylic methyl signals and the large vicinal coupling constant across the C-10/C-11 double

bond indicate that the olefins in **2** are all of (*E*)-geometry. ROESY correlations are fully consistent with this conclusion.

To determine the solution conformation of isoapoptolidin, representative ROESY correlations were used to evaluate the results of a Monte Carlo conformational search using Macromodel 7.0.⁶ Of the 51 ROESY correlations resolved for the C-1 to C-26 portion of isoapoptolidin, 23 were nontrivial and applied in the subsequent analysis. Strong ROESY correlations are observed between 3-H and 5-H and between 5-H and 7-H, indicating that the three methyl groups on the triene lie on the same face of the macrolide as they do in apoptolidin. Particularly notable are transannular correlations between 3-H and both 18-H_β and 15-H_β. The observed hypsochromic shift in the enoate chromophore from a λ_{max} of 319 nm in **1** to 304 nm in **2**, along with a decrease in the extinction coefficient for this absorption, from 22 800 in **1** to 19 400 in **2**, suggests a decrease in the degree of conjugation for the triene system in **2** relative to **1**.

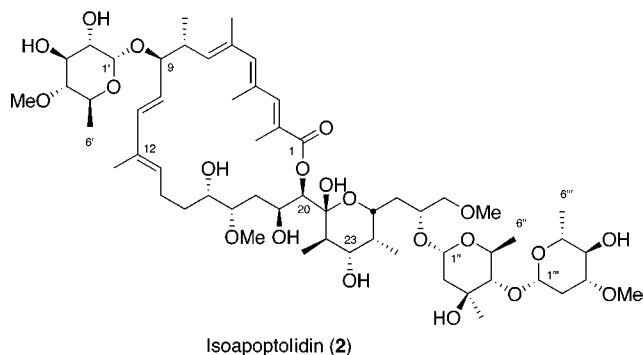


Figure 1. Structure and numbering scheme for isoapoptolidin.

The unusually high chemical shift of 19-H in **2** could be attributed to a new hydrogen bond between the C-19 alcohol and the C-25 oxygen. Significant ROESY correlations between the 20-H and the 22-H proton suggest an arrangement of the C-20/C-21 torsion that would favor this hydrogen bond. A representative structure from the conformational

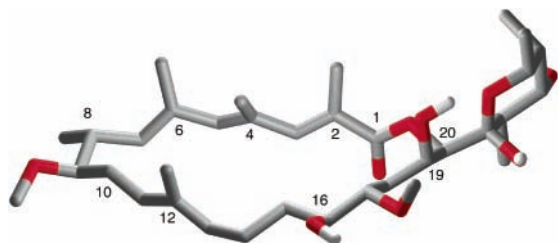


Figure 2. Representative solution conformation of the region from C-1 to C-26 of **2**, excluding 6-deoxy-4-*O*-methyl-L-glucose, oleandrose, and olivomycose residues.

search is depicted in Figure 2⁷ and is fully consistent with data from the ROESY experiment.

The identification of isoapoptolidin raises the possibility that an interconversion between **1** and **2** could take place under the conditions of biological assay or chemical isolation. Apoptolidin has been found to be stable for up to three months at $-20\text{ }^{\circ}\text{C}$ when dissolved in chloroform or methylene chloride. During this time, no conversion to isoapoptolidin can be observed, either by NMR or HPLC. Similarly, isoapoptolidin is stable as a solution in methanol at $-20\text{ }^{\circ}\text{C}$ for up to six months. In contrast, a dilute aqueous solution of apoptolidin at ambient temperature can be observed to convert to isoapoptolidin when monitored by HPLC or UV-vis. Similarly, an aqueous solution of **2** can be observed to convert to **1**. The respective products of these conversions can be isolated and are found to be **2** and **1**. Because this conversion goes in both directions, **1** and **2** are likely to be in simple equilibrium.

For synthetic work and for the evaluation of biological assays of apoptolidin and its derivatives, it is critical that the equilibrium constant and rates of interconversion are known under relevant conditions. To measure these kinetic parameters, solutions of **1** and **2** in Dulbecco's phosphate-buffered saline⁸ (PBS) were prepared and incubated at $37\text{ }^{\circ}\text{C}$ in sealed reaction vessels. Periodically, the components present in these solutions were quantified using reverse-phase HPLC.⁹ After normalization for the difference in extinction coefficients ($\lambda_{\text{obs}} = 254\text{ nm}$), these values were plotted (Figure 3), and the rate constants k_1 and k_{-1} were extracted

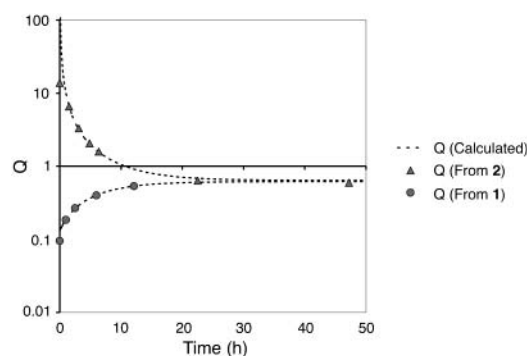


Figure 3. Kinetics toward equilibrium for the interconversion of **1** and **2** in aqueous solution where $Q = [2]/[1]$.

by fitting the data to the integrated rate expression for a simple equilibrium (Table 2).

The rate parameters calculated starting from either a solution of **1** or a solution of **2** are very similar, suggesting

- (4) (a) Schuppan, J.; Wehlan, H.; Keiper, S.; Koert, U. *Angew. Chem., Int. Ed.* **2001**, *40*, 2063. (b) Schuppan, J.; Ziemer, B.; Koert, U. *Tetrahedron Lett.* **2000**, *41*, 621. (c) Toshima, K.; Arita, T.; Kato, K.; Tanaka, D.; Matsumura, S. *Tetrahedron Lett.* **2001**, *42*, 8873. (d) Nicolaou, K. C.; Li, Y.; Fylaktakidou, K. C.; Mitchell, H. J.; Wei, H. X.; Weyershausen, B. *Angew. Chem., Int. Ed.* **2001**, *40*, 3849. (e) Nicolaou, K. C.; Li, Y.; Fylaktakidou, K. C.; Mitchell, H. J.; Sugita, K. *Angew. Chem., Int. Ed.* **2001**, *40*, 3854. (f) Nicolaou, K. C.; Li, Y.; Weyershausen, B.; Wei, H. X. *Chem. Commun.* **2000**, 307. (g) Sulikowski, G. A.; Jin, B. H.; Lee, W. M.; Wu, B. *Abstracts of Papers*, 218th National Meeting of the American Chemical Society, New Orleans, LA, Aug 22–26, 1999; American Chemical Society: Washington, DC, 1996; 563-ORGN. (h) Sulikowski, G. A.; Jin, B. H.; Lee, W. M.; Wu, B. *Org. Lett.* **2000**, *2*, 1439.

Table 2. Kinetic Parameters for the Equilibrium of **1** and **2** in Dulbecco's PBS at 37 °C^a

$$\text{Apoptolidin (1)} \xrightleftharpoons[k_{-1}]{k_1} \text{Isoapoptolidin (2)}$$

	$Q(t) = 0$ at $t = 0$	$Q(t) = \infty$ at $t = 0$
k_1	0.0656 h ⁻¹	0.0626 h ⁻¹
k_{-1}	0.106 h ⁻¹	0.0982 h ⁻¹
K_{eq}	0.616	0.638

^a $Q(t) = [2]/[1]$ at time t .

the absence of any long-lived intermediate structure. Furthermore, an equilibrium constant of ~ 0.6 suggests that the isolation yields of **1** and **2** are governed by this interconversion. More importantly, the value of k_1 suggests that under the conditions of most cell-based assays, a significant conversion of **1** to **2** will have occurred within several hours.¹⁰ The presence of isoapoptolidin, therefore, must be taken into account when interpreting the results of cell-based assays.

As a preliminary assessment of the biological activity of **2**, its ability to inhibit F₀F₁-ATPase in isolated yeast mitochondria was measured.¹¹ The duration of this assay is less than 20 min, during which time the isomerization of **1** and **2** should be minimal. To ensure that this is the case,

(5) In a typical procedure, 1.0 g of cell extract was purified using a 40 cm \times 2.5 cm flash column of 230–400 mesh normal-phase silica eluting with 7% methanol in chloroform.

(6) (a) Mohamadi, F.; Richards, N. G. J.; Guida, W. C.; Liskamp, R.; Lipton, M.; Caulfield, C.; Chang, G.; Hendrickson, T.; Still, W. C. *J. Comput. Chem.* **1990**, *11*, 440. (b) Calculations performed using the GB/SA water solvation model: Still, W. C.; Tempczyk, A.; Hawley, R. C.; Hendrickson, T. *J. Am. Chem. Soc.* **1990**, *112*, 6127.

(7) Image rendered using VMD-Visual Molecular Dynamics: Humphrey, W.; Dalke, A.; Schulten, K. *J. Mol. Graphics* **1996**, *14*, 33.

(8) Dulbecco, R.; Vogt, M. *J. Exp. Med.* **1957**, *106*, 167.

solutions of **1** and **2** including all assay components were analyzed for isomerization. After 20 min at 37 °C, less than 12% conversion was detected for either compound.

These data indicate that apoptolidin is a more potent inhibitor of F₀F₁-ATPase than isoapoptolidin (Table 3). It is

Table 3. Results of the F₀F₁-ATPase Inhibition Assay for **1** and **2**

	IC ₅₀ (μM)
apoptolidin (1)	0.7 ± 0.5
isoapoptolidin (2)	17 ± 5

not clear, however, if this difference in inhibitory activity can be extended to infer differences in the desired biological effect of apoptolidin: the selective induction of apoptosis. It is critical to determine which structure is more relevant, and to what degree, in order for an understanding of the structural basis for activity to be meaningful or useful. Experiments that address this issue are currently underway.

Acknowledgment. This research was supported by a grant (CA31845) from the National Cancer Institute. We thank Professor Chaitan Khosla for his guidance with the ATPase inhibition assay and isolation of apoptolidin.

Supporting Information Available: Experimental procedure for the ATPase inhibition assay and spectroscopic data for **2**, including ¹H NMR, ¹³C NMR, DQF-COSY, HSQC, HMBC, ROESY, IR, and ESMS. This material is available free of charge via the Internet at <http://pubs.acs.org>.

OL0266222

(9) Baseline separation can be achieved using a 150 \times 4.6 mm C18/5 μ column eluting with a water/acetonitrile gradient from 40% to 90% over 30 min.

(10) The half-life for k_1 in the absence of k_{-1} is 10.5 h.

(11) Roberts, H.; Choo, W. M.; Murphy, M.; Marzuki, S.; Lukins, H. B.; Linnane, A. W. *FEBS Lett.* **1979**, *108*, 501.